Biochemistry and Biophysics Reports 11 (2017) 93–98

Contents lists available at ScienceDirect

Biochemistry and Biophysics Reports

journal homepage: www.elsevier.com/locate/bbrep

Indispensable residue for uridine binding in the uridine-cytidine kinase family

Fumiaki Tomoike[a,b], Noriko Nakagawa[c], Kenji Fukui[d], Takato Yano[d], Seiki Kuramitsu[c], Ryoji Masui[e,*]

[a] Graduate School of Frontier Biosciences, Osaka University, 1-3 Yamadaoka, Suita, Osaka 565-0871, Japan
[b] Research Center for Materials Science, Nagoya University, Furo-Cho, Chikusa-ku, Nagoya 464-8602, Japan
[c] Department of Biological Sciences, Graduate School of Science, Osaka University, 1-1 Machikaneyama-cho, Toyonaka, Osaka 560-0043, Japan
[d] Department of Biochemistry, Osaka Medical College, 2-7 Daigakumachi, Takatsuki, Osaka 569-8686, Japan
[e] Graduate School of Science, Osaka City University, 3-3-138 Sugimoto, Sumiyoshi-ku, Osaka 558-8585, Japan

ARTICLE INFO

Keywords:
Uridine-cytidine kinase
Substrate specificity
Crystal structure
Nucleotide metabolism
Thermus thermophilus

ABSTRACT

Uridine-cytidine kinase (UCK), including human UCK2, are a family of enzymes that generally phosphorylate both uridine and cytidine. However, UCK of *Thermus thermophilus* HB8 (ttCK) phosphorylates only cytidine. This cytidine-restricted activity is thought to depend on Tyr93, although the precise mechanism remains unresolved. Exhaustive mutagenesis of Tyr93 in ttCK revealed that the uridine phosphorylation activity was restored only by replacement of Tyr93 with His or Gln. Replacement of His117 in human UCK2, corresponding to residue Tyr93 in ttCK, by Tyr resulted in a loss of uridine phosphorylation activity. These findings indicated that uridine phosphorylation activity commonly depends on a single residue in the UCK family.

1. Introduction

Nucleotides are critically important for all living cells because they are a source of nucleic acids, coenzymes and energy. Almost all organisms have two pathways for the synthesis of nucleotides; the *de novo* and salvage pathways. Living systems favor the more energy-efficient salvage pathway, which utilizes the degradation products of nucleotides and nucleic acids, over the *de novo* pathway [1]. Under some conditions or in some types of cells, nucleotide precursors are predominantly supplied *via* the salvage pathway. In addition, some therapeutic drugs are converted *in vivo* into compounds with anticancer effects possibly due to inhibition of DNA replication *via* the salvage pathway. Therefore, the salvage pathway enzymes have been a focus of constant attention in the development of anticancer and antiparasitic drugs [2,3].

Uridine-cytidine kinase (UCK) is one of the enzymes in the nucleoside salvage pathway [4]. UCK generally converts both cytidine and uridine to nucleoside monophosphate using ATP as the phosphate donor [5–7]. UCK is known to be overexpressed in tumor cells [8] and is also involved in the potency of several anticancer drugs [2]. The 3-D structure and reaction mechanism of UCK have been extensively studied [9–12]. However, the mechanism of substrate recognition remains obscure. UCK of *Thermus thermophilus* HB8 (ttCK) has been reported to display activity with cytidine only [11]. Uridine was thought to be unable to bind to ttCK because uracil, uridine, UMP and UTP exhibited no inhibition of ttCK activity. Structural comparison of ttCK with human UCK 2 (hsUCK2) [10], an archetypal UCK, suggested that the cytidine-limited specificity of ttCK depended on a single amino-acid residue, Tyr93 (Fig. 1) [11]. Moreover, the residue corresponding to Tyr93 of ttCK is His in many other UCKs, which is exemplified by hsUCK2. The replacement of Tyr93 in ttCK by His enabled ttCK to phosphorylate uridine, consistent with the expectation based on structural comparison [11]. However, the contribution of the 93rd residue of ttCK in terms of its substrate specificity remains elusive.

In this study, we replaced Tyr93 of ttCK with all other naturally occurring amino-acid residues and also replaced the corresponding His residue (His117) in hsUCK2 with Tyr, and assessed the kinetic properties of each purified mutant enzyme for uridine and cytidine. Based on the results, together with the model structures of ttCK mutants-uridine complexes, we hypothesized that the interaction between the 93rd residue and the O4 atom of uracil was indispensable for the activity toward uridine.

Abbreviations: UCK, uridine-cytidine kinase; ttCK, UCK (TTHA0578) in *T. thermophilus* HB8; hsUCK2, *Homo sapiens* UCK 2

* Corresponding author.
E-mail addresses: tomoike@chem.nagoya-u.ac.jp (F. Tomoike), naka5@bio.sci.osaka-u.ac.jp (N. Nakagawa), k.fukui@osaka-med.ac.jp (K. Fukui), med013@osaka-med.ac.jp (T. Yano), kuramitu@bio.sci.osaka-u.ac.jp (S. Kuramitsu), rmasui@sci.osaka-cu.ac.jp (R. Masui).

http://dx.doi.org/10.1016/j.bbrep.2017.07.002
Received 24 November 2016; Received in revised form 9 June 2017; Accepted 3 July 2017
Available online 08 July 2017

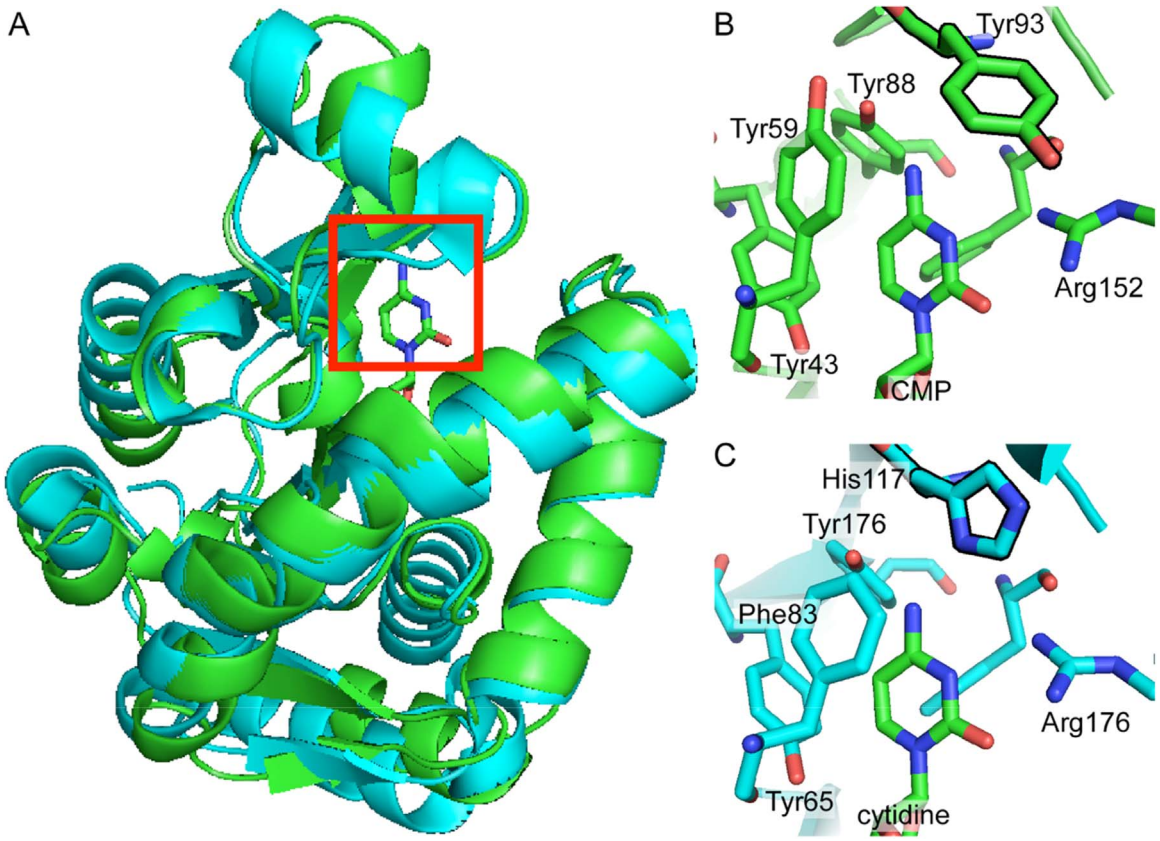

Fig. 1. Structures of ttCK and hsUCK2. Green and blue indicate CMP-complex structure of ttCK (PDB ID: 3ASZ) and cytidine-complex structure of hsUCK2 (PDB ID: 1UEJ), respectively. Panel (A) shows the comparison of the subunit structures. Red box indicates the recognition site for the nucleoside base. Panels (B) and (C) show close-up views of the base-recognition site of ttCK and hsUCK2, respectively. Thick lines emphasize Tyr93 of ttCK and His117 of hsUCK2.

2. Materials and methods

2.1. Site-directed mutagenesis

Site-directed mutagenesis of ttCK and hsUCK2 was performed by using the method of Iwai et al. [13] with some modifications. Briefly, a point mutation was inserted into the gene of ttCK or hsUCK2 by means of the inverse PCR method. PCR was performed using KOD DNA polymerases (Toyobo) and expression plasmid containing the respective gene as a template. PCR reaction solution contained 400 nM primers, 2.5 mM $MgCl_2$, 0.2 mM dNTP, expression plasmid, and KOD enzyme. The sequences of chemically synthesized primers (BEX) are summarized in Table 1. The sequences of expression plasmids for ttCK mutants and H117Y hsUCK2 mutant were confirmed.

2.2. Protein overexpression and purification

The expression plasmids for ttCK mutants were transformed into *Escherichia coli* Rosetta(DE3). The transformants were cultured at 37 °C in 1.5 L of LB medium supplemented with 50 μg mL^{-1} of ampicillin for 12 h. Cells were harvested by centrifugation. ttCK was purified by heat treatment at 70 °C for 20 min and column chromatography with

Table 1
Sequences of primers for PCR.

Mutation	Forward primer (5′–3′)	Reverse primer (5′–3′)
ttCK		
Y93W	GCCTGGACCCGAAGCC	CCCCTTTCCAGGACGT
Y93I	GCCATCACCCGAAGCCC	CCCCTTTCCAGGACGT
Y93V	GCCGTCACCCGAAGCC	CCCCTTTCCAGGACGT
Y93P	GCCCCCACCCGAAGC	CCCCTTTCCAGGACGT
Y93A	GCCGCCACCCGAAGC	CCCCTTTCCAGGACGT
Y93G	GCCGGCACCCGAAGC	CCCCTTTCCAGGACGT
Y93T	GCCACCACCCGAAGCCCCAG	CCCCTTTCCAGGACGT
Y93S	GCCTCCACCCGAAGCC	CCCCTTTCCAGGACGT
Y93M	GCCATGACCCGAAGCCCCAG	CCGGAAGTCGTAGACGGGCATCT
Y93C	GCCTGCACCCGAAGCC	CCCCTTTCCAGGACGT
Y93N	GCCAACACCCGAAGCCC	CCCCTTTCCAGGACGT
Y93E	GCCGAAACCCGAAGCCC	CCCCTTTCCAGGACGT
Y93D	GCCGACACCCGAAGCC	CCCCTTTCCAGGACGT
Y93R	GCCCGCACCCGAAGC	CCCCTTTCCAGGACGT
Y93K	GCCAAAACCCGAAGCCCCAGA	CCGGAAGTCGTAGACGGGCATCT
hsUCK2		
H117Y	TCTCCTATTCCCGGAAGAGGAGA	CAAAGTCATACACGGGGATCTGGACT

Toyopearl Phenyl 650 M (Tosoh), Toyopearl SP-650 column (Tosoh), and Superdex 200 10/300 GL column (GE Healthcare Biosciences). The expression plasmid for GST-fusion hsUCK2 (wild type (WT)) and its mutant (H117Y) were transformed into *E. coli* BL21(DE3). The transformants were cultured at 37 °C in 1.5 L of LB medium supplemented with 50 μg mL^{-1} of ampicillin for 12 h. Cells were harvested by centrifugation. hsUCK2 was purified by the column chromatography with GSTrap FF (GE Healthcare Biosciences). The concentrations of the purified ttCK variants were determined by using molar absorption coefficients at 278 nm, calculated to be 11,200 for ttCK variants except ttCK (Y93W) and 16,800 M^{-1} cm^{-1} for ttCK (Y93W) [11].

2.3. Enzyme assay

The k_{cat} and K_M values of ttCK and hsUCK2 variants for cytidine and uridine were determined by using an NADH-dependent enzyme-coupled assay [14] with a UV spectrophotometer, U-3000 (Hitachi). Measurements were performed at 25 °C in solutions containing 20 mM HEPES (pH 7.2), 100 mM KCl, 2 mM $MgCl_2$, 50–2000 μM cytidine, 100–200 μM ATP, 15 μM NADH, 15 μM phosphoenolpyruvate, 0.5 mU of lactate dehydrogenase from pig heart (Toyobo), 0.5 mU of pyruvate kinase from rabbit muscle (Sigma) and 0.15 μM ttCK. The concentration of ATP was the concentration when ttCK had the highest activity towards cytidine. The kinetic constants, k_{cat} and K_M, were determined by fitting the data to Michaelis-Menten equation with IGOR Pro ver. 4.0.3.0 (WaveMetrics).

Reversed-phase HPLC was used to identify reaction products. The reaction mixture contained 20 mM Tris-HCl, 100 mM KCl, 10 mM $MgCl_2$, 50 μM each nucleoside (adenosine, guanosine, uridine, cytidine, deoxyadenosine, deoxyguanosine, thymidine, and deoxycytidine), 500 μM ATP, and 50 nM ttCK at pH 8.0. The reaction mixtures were incubated at 25 °C or 37 °C for 1 h. The reaction products were separated by a CAPCELL PAK C18 column (Shiseido).

2.4. Crystallization, data collection and structure determination

The protein solution for crystallization of a ternary complex of Y93H contained 19.3 mg/mL Y93H ttCK, 20 mM cytidine, and 2 mM adenosine β,γ-methyleneadenosine 5′-triphosphate (AMPPCP). The crystals were obtained in a solution of 50% of No 46 (0.1 M sodium chloride, 0.1 M BICINE, pH 9.0, 20% (v/v) polyethylene glycol monomethyl ether 550) from Crystal screen II (HAMPTON). Data were collected with the RIKEN Structural Genomics Beamline II (BL26B2) [15] at SPring-8 (Hyogo, Japan). Data were processed by using the HKL-2000 program suite [16]. Structures were solved by using a molecular replacement method with Molrep [17]. The coordinates of ternary complex of WT ttCK, cytidine, and AMPPCP (PDB ID: 3W34) [12] were used as the starting model. Model refinement was carried out by using the programs CCP4 [18] and Coot [19]. According to PROCHECK [20], the final models have 89.0% of their residues in the most favored region of the Ramachandran plot, and no residues were found in the forbidden regions for either structure. The data-collection statistics and processed data statistics are presented in Table 2. The determined structure was deposited in Protein Data Bank ~~as~~ (PDB ID: 3W8R). The molecular graphics were prepared with Chimera [21].

2.5. Docking simulation

We examined the influence of amino acid substitution at Tyr93 of ttCK on substrate binding by docking simulation using Molecular Operating Environment software version 2014.10 (MOE 2014.10. Chemical Computing Group Inc.). Docking simulation of WT or Y93H ttCK with uridine was calculated using MOE 2014.10. First, for Y93Q, Y93N, Y93K and Y93R, ligand-free structures were generated from the ligand-free form of WT ttCK by replacing Tyr93 using Mutate Residue functionality. For WT and Y93H, the structures of cytidine-bound form (PDB ID: 3W34 and 3W8R, respectively) were used. Then, the energy-minimized structures of respective ttCKs with hydrogen atoms were prepared with the AMBER10:EHT force field and implicit Born solvation. The ligand-binding sites were defined by the Site Finder application in MOE and docking simulations were carried out using ASEDock [22]. The lowest energy conformations with the smallest energies (U_{dock} and U_{total} values) were obtained nine times. The U_{total} and U_{dock} values were utilized for the evaluation of the protein-ligand interaction. U_{total} (kcal/mol) is the sum of U_{ele} (electrostatic energy), U_{vdw} (van der Waals energy), U_{solv} (solvation energy) and U_{ligand} (ligand energy). U_{dock} (kcal/mol) is the sum of U_{ele}, U_{vdw}, U_{solv} and U_{strain} (strain energy).

Table 2
Data collection and refinement statistics for Y93H ttCK in complex with cytidine and AMPPCP.

Crystal parameters	
Space group	$P2_12_12$
Unit cell parameters	
a (Å)	68.290
b (Å)	124.103
c (Å)	60.731
α = β = γ (°)	90
Data processing	
Resolution range	23.04–2.49
No. of used reflection	1,133,267
Completeness (%)	94.7 (94.1)[c]
Redundancy	5.6 (5.2)
$I/\sigma(I)$	25.7 (4.8)
R_{merge} (%)[a]	8.6 (36.1)
Refinement parameters	
Resolution range	23.04–2.49
Number of reflection	16,731
R factor[b]	0.202
R_{free} factor	0.292
No. of atom	
Protein	3,285
Water	47
Metal ion	1
Ligand	96
Average B value (Å^2)	38.987
Root mean square deviations	
Bond lengths (Å)	0.034
Bond angles (°)	2.76
Ramachandran plot (%)	
Most favored	89.0
Additional allowed	10.4
Generously allowed	0.6
Disallowed	0.0

[a] $R_{merge} = \Sigma_{hkl} \Sigma_i |I_i(hkl) - \langle I(hkl)\rangle| / \Sigma_{hkl} \Sigma_i I_i(hkl)$, where $\langle I(hkl)\rangle$ is the average of individual $I_i(hkl)$ measurements.
[b] $R = ||F_0| - |F_c|/\Sigma|F_0|$.
[c] Values in parentheses are for the outermost shell.

3. Results and discussion

To elucidate the detailed contribution of this residue to substrate specificity, Tyr93 in ttCK was replaced by all other naturally occurring amino-acid residues. All mutant proteins were successfully overexpressed in *E. coli* and then purified to homogeneity. The phosphorylation activities of these mutants toward uridine and cytidine were measured by using an NADH-dependent enzyme-coupled assay (Table 3). Among all 19 mutants, only the Y93H mutant restored significant phosphorylation activity for uridine, which was comparable to its activity toward cytidine. Phosphorylation of cytidine and uridine by Y93H was confirmed by HPLC analysis (Fig. 2). The kinetic constants for uridine could be determined only using Y93H and Y93Q. Nonetheless, the k_{cat}/K_M value of Y93Q for uridine was less than a tenth that of Y93H. All the other mutants exhibited very low activity toward uridine. The k_{cat}/K_M values of Y93W, Y93R and Y93K for uridine could not be determined. The k_{cat}/K_M values of the other mutants for uridine were less than a tenth of those for cytidine. In particular, the uridine phosphorylation by WT and Y93W was not detected even after prolonged incubation time,

Table 3
Kinetic parameters of ttCK and hsUCK2 mutants[a].

Enzyme	Cytidine			Uridine		
	k_{cat} (s^{-1})	K_M (μM)	k_{cat}/K_M ($M^{-1}\,s^{-1}$)	k_{cat} (s^{-1})	K_M (μM)	k_{cat}/K_M ($M^{-1}\,s^{-1}$)
ttCK						
WT[b]	4.1 ± 0.8	72 ± 24	5.7×10^4	–[c]	–	–
Y93H[b]	8.4 ± 1.1	220 ± 27	3.8×10^4	9.2 ± 1.7	360 ± 43	2.6×10^4
Y93W	0.4 ± 0.1	71 ± 23	6.0×10^3	–	–	–
Y93F[b]	5.9 ± 1.7	100 ± 49	5.7×10^4	n. d.[d]	n. d.	1.6×10
Y93L[b]	10 ± 4	420 ± 11	2.4×10^4	n. d.	n. d.	1.5×10^2
Y93I	2.9 ± 0.3	574 ± 34	5.1×10^3	n. d.	n. d.	9.2×10
Y93V	3.9 ± 0.2	965 ± 52	4.1×10^3	n. d.	n. d.	7.9×10
Y93P	4.6 ± 0.9	555 ± 99	8.3×10^3	n. d.	n. d.	9.7×10
Y93A	4.5 ± 0.8	383 ± 63	1.2×10^4	n. d.	n. d.	5.1×10
Y93G	2.9 ± 0.2	620 ± 70	4.6×10^3	n. d.	n. d.	4.3×10
Y93T	3.1 ± 0.1	587 ± 33	5.3×10^3	n. d.	n. d.	6.1×10^2
Y93S	7.1 ± 0.6	225 ± 43	3.2×10^4	n. d.	n. d.	2.9×10^2
Y93M	7.2 ± 0.6	950 ± 74	7.7×10^3	n. d.	n. d.	4.8×10
Y93C	1.9 ± 0.4	215 ± 80	9.0×10^3	n. d.	n. d.	2.3×10
Y93Q[b]	2.8 ± 0.5	230 ± 33	1.2×10^4	1.1 ± 0.4	1600 ± 590	7.2×10^2
Y93N	4.1 ± 0.8	470 ± 123	8.7×10^3	n. d.	n. d.	4.1×10
Y93E	1.5 ± 0.1	186 ± 35	5.8×10^3	n. d.	n. d.	5.6×10
Y93D	1.4 ± 0.6	236 ± 16	5.8×10^3	n. d.	n. d.	5.6×10
Y93R	–	–	–	–	–	–
Y93K	–	–	–	–	–	–
hsUCK2						
WT	4.3 ± 0.2	42 ± 12	1.0×10^5	5.2 ± 0.5	58 ± 1.7	9.0×10^4
H117Y	6.4 ± 0.7	138 ± 15	4.7×10^4	n. d.	n. d.	9.6×10^2

[a] Measurements were performed at 25 °C in solutions containing 20 mM HEPES (pH 7.2), 100 mM KCl, 2 mM $MgCl_2$, 50–2000 μM cytidine, 100–200 μM ATP, 15 μM NADH, 15 μM phosphoenolpyruvate, 0.5 mU of lactate dehydrogenase, 0.5 mU of pyruvate kinase and 0.15 μM ttCK.
[b] These parameters were reported in our previous study [11].
[c] Dashes indicate no detectable activity.
[d] n.d.: not determined.

although they were active toward cytidine. Y93R and Y93K were inactive for both cytidine and uridine. These mutagenesis analyses indicated that only His and Gln residues at the 93rd position of ttCK enabled the enzyme to accept uridine as a substrate.

3.1. Structural analysis of Y93H ttCK with substrates

To elucidate the reason for the acceptance of uridine by Y93H ttCK, crystal structure of Y93H with cytidine and AMPPCP, a non-hydrolysable ATP analogue, was determined at a resolution at 2.5 Å. Overall structure in the asymmetric unit is shown in Fig. 3. In the crystals, the asymmetric unit contained two Y93H molecules. Furthermore, two dimers of Y93H can be related by a crystallographic symmetry operation, suggesting that Y93H exists as a tetramer in the crystal lattice. These are the same as the WT ttCK crystals [11,12]. Each subunit is composed of seven α-helices and six β-strands. Four-stranded β-sheet is sandwiched by four α-helices, and this core domain forms the ATP-binding site. In the electron density, only the phosphate moiety of AMPPCP was detected as well as WT ttCK [12]. Cytidine is bound in the pocket formed by the LID, β hairpin and NMP-binding domains. These indicate that the overall structure of Y93H is almost the same as that of WT ttCK.

Location of residues involved in the interaction with cytidine in Y93H is identical to that in WT enzyme except for Tyr93 (Fig. 4(B)). The Nδ1 atom of His93 in the Y93H structure forms a hydrogen bond with the N4 atom of bound cytidine (Fig. 4(A)). This interaction is similar to that of His117 in hsUCK2 structure [10] (Fig. 4(A)). Interactions between cytidine and residues other than His93 in Y93H resemble those in hsUCK2. Although the N4 atom of cytosine is replaced by an oxygen atom for uracil, His117 in hsUCK2 can form a hydrogen bond with uracil as a proton donor [10]. These suggest that His93 is solely responsible for the acceptance of uridine by Y93H ttCK.

Based on the structural analysis of the Y93H-cytidine complex, the activity of Y93Q toward uridine implies a hydrogen bond between the side-chain amino group of Gln93 and the O4 atom of bound uracil. Similarly, the weak activities of Y93T and Y93S toward uridine imply the interaction of the O4 atom of uracil with the side-chain hydroxyl

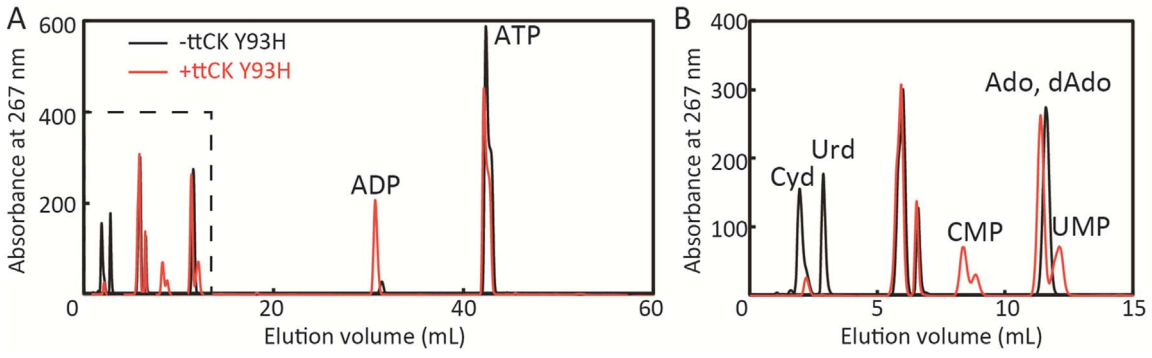

Fig. 2. HPLC analysis of Y93H reaction products. Whole and expanded chromatograms are shown in panel A and B, respectively. Detailed experimental conditions are described in Section 2. Note that CMP standard sample was eluted as a doublet under this condition.

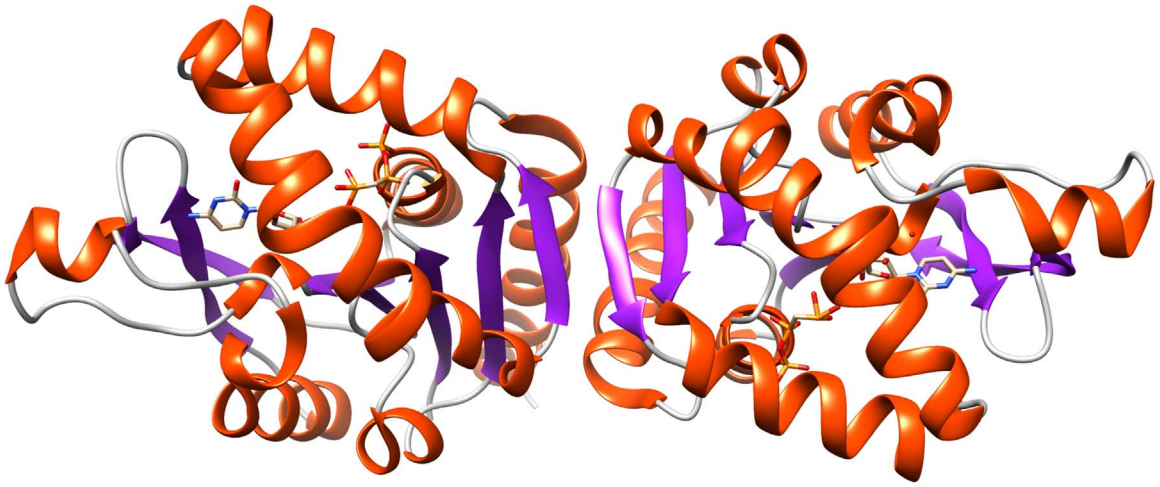

Fig. 3. Overall structure of Y93H ttCK with cytidine. Secondary structures, α-helices and β-sheets, are shown in red and purple, respectively. Ball and stick models exhibit substrates, cytidine and AMPPCP models, and residues, interacting the substrates.

groups of Thr93 and Ser93, respectively. The observation that Y93N showed lower activity toward uridine than Y93Q suggests that the length of Asn side chain is insufficient to form a hydrogen bond with the O4 atom of uridine and the side-chain amino-group of Asn93. In addition, the structures suggest that the Arg152 forms the hydrogen bond with uridine. The replacement of Arg152 with Leu reduced the activity towards cytidine (data not shown). These interactions between uridine and ttCK are indispensable for substrate binding, which is consistent with the molecular dynamics simulation [23].

The importance of a hydrogen bond with the O4 atom of uracil seems to be consistent with other enzymes such as UMP kinase [24], thymidine phosphorylase [25,26], TMP kinase [27] and UDP-glucose 6-dehydrogenase [28]. These enzymes form a hydrogen bond between the O4 atom of uracil or thymine moiety of substrate and a basic residue: His in UMP kinase, Arg in thymidine phosphorylase and TMP kinase, and Lys in UDP-glucose 5-dehydrogenase. It should be noted, however, that the necessity of these interactions for base recognition has not been proved. In UMP-CMP kinase, the O4 atom of the uracil moiety forms a hydrogen bond with a water molecule, which interacts with the side chains of Asn and Arg [29]. This may explain why the k_{cat}/K_M values of Y93S and Y93T toward uridine were relatively high (of the order of 10^2) compared with other mutants with low uridine phosphorylation activity (of the order of 10). Although the side chains of Ser and Thr are too short to form a direct hydrogen bond with uracil, it is possible that these residues interact with uracil *via* a water molecule.

Except for Y93R and Y93K, the activities of ttCK mutants toward cytidine were high enough to determine the kinetic constants (Table 3), which may provide some information about the contribution of the 93rd residue in terms of substrate binding. The introduction of large side-chain residues, such as Tyr (WT), Trp and Phe, gave relatively small K_M values (approximately 100 μM). This finding suggests that the bulky side chains reduce the spatial volume within the nucleoside-binding site and thereby stabilize the substrate-binding state. The relatively small K_M value (220 μM) of Y93H might be explained by the same mechanism. The replacement of Tyr93 with Asp, Glu, Gln, Ser and Cys also furnished ttCK K_M values comparable to that of Y93H (approximately 200 μM). These residues can presumably interact with cytidine because their side chains can form a hydrogen bond. In contrast, replacement of Tyr93 with aliphatic hydrophobic residues, Pro or Gly generally resulted in larger K_M values, probably due to their inability to form hydrogen bonds. Nonetheless, it is difficult to explain why Y93T and Y93N gave relatively high K_M values (approximately 500 μM).

To further verify the hypothesis that significant activity of UCK for uridine requires His at position 93, His117 of hsUCK2, the corresponding residue to Tyr93 of ttCK (Fig. 1(C)), was replaced with Tyr.

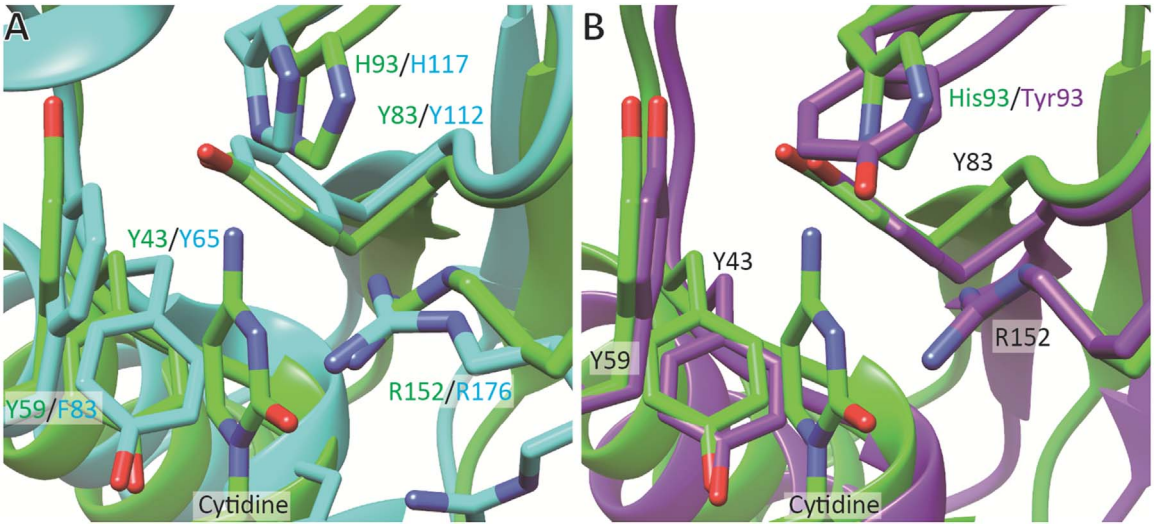

Fig. 4. Nucleoside-binding site of Y93H ttCK. Panel (A) shows the comparison between Y93H ttCK mutant (green) and WT hsUCK2 (blue). Panel (B) shows the comparison between WT (purple) and Y93H (green) ttCK.

HsUCK2 displays activity toward both cytidine and uridine [7,30] and its structure has been determined [10]. Whereas the activities of WT hsUCK2 toward uridine and cytidine were equivalent as expected, the activity of H117Y toward uridine was severely diminished (Table 3). From these results, it can be concluded that the mutation of His117 had no effect on the kinetic mechanism and affected only the activity toward uridine. This finding supports our hypothesis and indicates that the dependence of substrate specificity on a single amino acid residue is a general characteristic of the UCK family of enzymes. If this conclusion is correct, the substrate specificity of UCK family proteins can be accurately predicted by simply determining the corresponding residue to Tyr93 of ttCK. It should be noted that the mutation Y93H of ttCK and H117Y of hsUCK2 both decreased the binding affinity of the respective enzyme for cytidine. This suggests that other amino-acid residue(s) beside Tyr93/His117 might contribute to the optimal substrate binding.

Finally, in order to find more clues to an indispensable factor for uridine phosphorylation activity of ttCK, the structures of the complex of ttCK mutants and uridine or cytidine were modeled by employing MOE using ttCK WT and Y93H structures. In the WT-cytidine structure, Tyr93 is located near the base of the bound ligand, but forms no interaction with it (Supplementary Fig. 1). MOE simulation suggested that WT ttCK also formed a stable complex with uridine although Tyr93 formed no interaction with uracil moiety. The calculated U_{dock} values (for the lowest energy conformation) are – 59 and − 60 kcal/mol for cytidine and uridine, respectively. Although at present we cannot present a rationale to explain this apparent discrepancy, this may imply the presence of critical but unidentified step in formation of ttCK-substrate complex. We further performed docking simulation for ttCK mutants. Y93H formed a stable complex with uridine as well as cytidine with similar U_{dock} values (– 65 and − 67 kcal/mol, respectively). In the modeled structure, the distance (3.5 Å) between the O4 atom of uracil and the imino group of His93 in Y93H was close to form a hydrogen bond (data not shown). In contrast, the distance between uracil and Gln93 in Y93Q was 4.7 Å, which is longer than that for His93, but shorter than that for Asn93 (5.3 Å) (Supplementary Fig. 2). This difference may explain why the activity for uridine of Y93Q was lower than Y93H but slightly higher than Y93N. Lys and Arg contain amino groups in their side chains, but their activities were undetectable not only for uridine but also for cytidine. In the model structures, however, substrate bound to the active sites of these mutants with similar U_{dock} values (approximately − 60 kcal/mol) (Supplementary Fig. 3)

In this study, it is clear that His in the base-binding site is indispensable for the activity of UCK family toward uridine. However, we are still uncertain why uridine cannot bind to UCK when this His residue is mutated. The K_M values for uridine of most mutants are expected to be decreased by more than two orders of magnitude. The proposed interaction between His and uracil alone seems insufficient to explain such a large decrease in binding affinity for this substrate. Further study is required to understand the full mechanism of this specificity.

Acknowledgements

We thank Drs. Nobuo N. Noda (Institute of Microbial Chemistry) and Dr. Fuyuhiko Inagaki (Hokkaido University) for generously providing of the expression plasmid of hsUCK2. This work was supported in part by the Japan Society for the Promotion of Science for Young Scientists (10J01804, FT).

Appendix A. Supplementary material

Supplementary data associated with this article can be found in the online version at http://dx.doi.org/10.1016/j.bbrep.2017.07.002.

Appendix A. Transparency document

Supplementary data associated with this article can be found in the online version at http://dx.doi.org/10.1016/j.bbrep.2017.07.002.

References

[1] D. Voet, J.G. Voet, Biochemistry, John Wiley & Sons, New York, 2010.
[2] D. Murata, Y. Endo, T. Obata, K. Sakamoto, Y. Syouji, M. Kadohira, A. Matsuda, T. Sasaki, A crucial role of uridine/cytidine kinase 2 in antitumor activity of 3′-ethynyl nucleosides, Drug Metab. Dispos. 32 (2004) 1178–1182.
[3] M.P. Postigo, R.V.C. Guido, G. Oliva, M.S. Castilho, I. da R. Pitta, J.F.C. de Albuquerque, A.D. Andricopulo, Discovery of new inhibitors of *Schistosoma mansoni* PNP by pharmacophore-based virtual screening, J. Chem. Inf. Model. 50 (2010) 1693–1705.
[4] M. Kilstrup, K. Hammer, P. Ruhdal Jensen, J. Martinussen, Nucleotide metabolism and its control in lactic acid bacteria, FEMS Microbiol. Rev. 29 (2005) 555–590.
[5] G.I. Deng, D.H. Ives, Non-allosteric regulation of the uridine kinase from seeds of *Zea mays*, Biochim. Biophys. Acta 377 (1975) 84–94.
[6] P. Valentin-Hansen, Uridine-cytidine kinase from *Escherichia coli*, Methods Enzymol. 51 (1978) 308–314.
[7] A.R. Van Rompay, A. Norda, K. Lindén, M. Johansson, A. Karlsson, Phosphorylation of uridine and cytidine nucleoside analogs by two human uridine-cytidine kinases, Mol. Pharmacol. 59 (2001) 1181–1186.
[8] A. Orengo, Regulation of enzymic activity by metabolites. I. uridine-cytidine kinase of Novikoff ascites rat tumor, J. Biol. Chem. 244 (1969) 2204–2209.
[9] A.J. Smith, Y. Li, K.N. Houk, Quantum mechanics/molecular mechanics investigation of the mechanism of phosphate transfer in human uridine-cytidine kinase 2, Org. Biomol. Chem. 7 (2009) 2716–2724.
[10] N.N. Suzuki, K. Koizumi, M. Fukushima, A. Matsuda, F. Inagaki, Structural basis for the specificity, catalysis, and regulation of human uridine-cytidine kinase, Structure 12 (2004) 751–764.
[11] F. Tomoike, N. Nakagawa, S. Kuramitsu, R. Masui, A single amino acid limits the substrate specificity of *Thermus thermophilus* uridine-cytidine kinase to cytidine, Biochemistry 50 (2011) 4597–4607.
[12] F. Tomoike, N. Nakagawa, S. Kuramitsu, R. Masui, Structural and biochemical studies on the reaction mechanism of uridine-cytidine kinase, Protein J. 34 (2015) 411–420.
[13] T. Iwai, S. Kuramitsu, R. Masui, The Nudix hydrolase Ndx1 from *Thermus thermophilus* HB8 is a diadenosine hexaphosphate hydrolase with a novel activity, J. Biol. Chem. 279 (2004) 21732–21739.
[14] K.C. Agarwal, R.P. Miech, R.E.J. Parks, Guanylate kinases from human erythrocytes, hog brain, and rat liver, Methods Enzymol. 51 (1978) 483–490.
[15] G. Ueno, H. Kanda, R. Hirose, K. Ida, T. Kumasaka, M. Yamamoto, RIKEN structural genomics beamlines at the SPring-8; high throughput protein crystallography with automated beamline operation, J. Struct. Funct. Genom. 7 (2006) 15–22.
[16] Z. Otwinowski, W. Minor, Processing of X-ray diffraction data collected in oscillation mode, Methods Enzymol. 276 (1997) 307–326.
[17] A. Vagin, A. Teplyakov, MOLREP: an automated program for molecular replacement, J. Appl. Cryst. 30 (1997) 1022–1025.
[18] Collaborative Computational Project, Number 4, The CCP4 suite: programs for protein crystallography, Acta Crystallogr. D Biol. Crystallogr. 50 (1994) 760–763.
[19] P. Emsley, B. Lohkamp, W.G. Scott, K. Cowtan, Features and development of Coot, Acta Crystallogr. D Biol. Crystallogr. 66 (2010) 486–501.
[20] R.A. Laskowski, M.W. MacArthur, D.S. Moss, J.M. Thornton, PROCHECK: a program to check the stereochemical quality of protein structures, J. Appl. Crystallogr. 26 (1993) 283–291.
[21] E.F. Pettersen, T.D. Goddard, C.C. Huang, G.S. Couch, D.M. Greenblatt, E.C. Meng, T.E. Ferrin, UCSF chimera – a visualization system for exploratory research and analysis, J. Comput. Chem. 25 (2004) 1605–1612.
[22] J. Goto, R. Kataoka, H. Muta, N. Hirayama, ASEDock-docking based on alpha spheres and excluded volumes, J. Chem. Inf. Model. 48 (2008) 583–590.
[23] W. Tanaka, M. Shoji, F. Tomoike, Y. Ujiie, K. Hanaoka, R. Harada, M. Kayanuma, K. Kamiya, T. Ishida, R. Masui, S. Kuramitsu, Y. Shigeta, Molecular mechanisms of substrate specificities of uridinecytidine kinase, Biophys. Physicobiol. 13 (2016) 77–84.
[24] C. Marco-Marin, F. Gil-Ortiz, V. Rubio, The crystal structure of *Pyrococcus furiosus* UMP kinase provides insight into catalysis and regulation in microbial pyrimidine nucleotide biosynthesis, J. Mol. Biol. 352 (2005) 438–454.
[25] R.A. Norman, S.T. Barry, M. Bate, J. Breed, J.G. Colls, R.J. Ernill, R.W. Luke, C.A. Minshull, M.S. McAlister, E.J. McCall, H.H. McMiken, D.S. Paterson, D. Timms, J.A. Tucker, R.A. Pauptit, Crystal structure of human thymidine phosphorylase in complex with a small molecule inhibitor, Structure 12 (2004) 75–84.
[26] M.J. Pugmire, W.J. Cook, A. Jasanoff, M.R. Walter, S.E. Ealick, Structural and theoretical studies suggest domain movement produces an active conformation of thymidine phosphorylase, J. Mol. Biol. 281 (1998) 285–299.
[27] I. Li de la Sierra, H. Munier-Lehmann, A.M. Gilles, O. Bârzu, M. Delarue, X-ray structure of TMP kinase from *Mycobacterium tuberculosis* complexed with TMP at 1.95 Å resolution, J. Mol. Biol. 311 (2001) 87–100.
[28] S. Egger, A. Chaikuad, K.L. Kavanagh, U. Oppermann, B. Nidetzky, Structure and mechanism of human UDP-glucose 6-dehydrogenase, J. Biol. Chem. 286 (2011) 23877–23887.
[29] K. Scheffzek, W. Kliche, L. Wiesmüller, J. Reinstein, Crystal structure of the complex of UMP/CMP kinase from *Dictyostelium discoideum* and the bisubstrate inhibitor P^1-(5′-adenosyl) P^5-(5′-uridyl) pentaphosphate (UP_5A) and Mg^{2+} at 2.2 Å: implications for water-mediated specificity, Biochemistry 35 (1996) 9716–9727.
[30] J.C. Drake, R.G. Stoller, B.A. Chabner, Characteristics of the enzyme uridine-cytidine kinase isolated from a cultured human cell line, Biochem. Pharmacol. 26 (1977) 64–66.